

Supplement of The Cryosphere, 13, 1297–1324, 2019
<https://doi.org/10.5194/tc-13-1297-2019-supplement>
© Author(s) 2019. This work is distributed under
the Creative Commons Attribution 4.0 License.



Supplement of

Challenges associated with the climatic interpretation of water stable isotope records from a highly resolved firn core from Adélie Land, coastal Antarctica

Sentia Goursaud et al.

Correspondence to: Sentia Goursaud (sentia.goursaud@lsce.ipsl.fr)

The copyright of individual parts of the supplement might differ from the CC BY 4.0 License.

5 **Table S1: Parameters of the linear relationship of the annual reconstructed accumulations including the only uncertain peak identified over the period cover by the stake data (2004-2014), as well as the original reconstructed accumulation given in the submitted version (“None”), with the SMB of the closest stake data than the drilling site (“19.2”) over the period 2004-2014: the slope (cm w.e. y^{-1} (cm w.e. y^{-1})⁻¹), the correlation coefficient (“r”), and the p-value and the standard error (“stderr”). The non-significant correlation between the reconstruction accumulation including the peak at 0.5 m w.e. and the SMB of the closest stake data than the drilling site lead us to exclude it from the dating.**

Depth (m w.e.)	r	pvalue
None	0.83	<0.05
0.5	0.16	0.64

5 **Table S2: Parameters of the linear relationship of the annual reconstructed accumulations including uncertain peaks identified by their depth along the core, and the original reconstructed accumulation given in the submitted version (“None”), with the simulated accumulation from the ECHAM5-wiso over the same cover period than the resulting reconstructions: the slope (cm w.e. y⁻¹ (cm w.e. y⁻¹)⁻¹), the correlation coefficient (“r”), and the p-value and the standard error (“stderr”). The line in bold highlights the reconstruction which gives the best correlation.**

Depth (m w.e.)	slope (cm w.e. y ⁻¹ (cm w.e. y ⁻¹) ⁻¹)	r	pvalue	stderr
None	0.28	0.45	0.07	0.22
6.8	0.03	0.06	0.82	0.20
12.5	0.20	0.36	0.14	0.42
6.8 and 12.5	-0.01	-0.02	0.93	0.14

Table S3: Parameters of the linear relationship of the annual $\delta^{18}\text{O}_{\text{TA}}$ including uncertain peaks identified by their depth along the core, and the annual $\delta^{18}\text{O}_{\text{TA}}$ given in the submitted version (“None”), with the $\delta^{18}\text{O}$ simulated by ECHAM5-wiso over the same cover period than the resulting reconstructions: the slope (‰‰^{-1}), the correlation coefficient (“r”), and the p-value and the standard error (“stderr”). The line in bold highlights the reconstruction which gives the best correlation.

Depth (m w.e.)	Slope (‰‰^{-1})	r	pvalue	stderr
None	0.16	0.32	0.21	0.12
6.8	0.11	0.28	0.25	0.09
12.5	0.18	0.37	0.14	0.11
6.8 and 12.5	0.11	0.27	0.26	0.09

5

Table S4: Total mean $\delta^{18}\text{O}$ seasonal amplitude (in ‰) and ratio of the three first years mean $\delta^{18}\text{O}$ seasonal amplitude by the mean $\delta^{18}\text{O}$ seasonal amplitude.

Station	Recorded period	Total mean seasonal amplitude (‰)	Ratio
GIP	2000-2007	15.1	1.2
BI	1996-2014	9.7	1.1
KM	1995-2014	7.0	1.5
KC	1958-2012	1.9	1.0
DSSA	1986-1992	8.0	1.2
NUS 08-7	1382-2008	0.8	8.7
WDC06A	-50-2005	1.8	2.9
IND25B5	1902-2006	4.4	1.2
TA192A	1998-2014	8.6	0.5

Table S5: Total mean deuterium excess seasonal amplitude (in ‰) and ratio of the three first years mean $\delta^{18}\text{O}$ seasonal amplitude by the mean $\delta^{18}\text{O}$ seasonal amplitude.

Station	Recorded period	Total mean seasonal amplitude (‰)	Ratio
GIP	2000-2007	17.8	1.4
BI	1996-2014	6.3	1.1
KM	1995-2014	5.5	1.4
KC	1958-2012	2.7	1.0
DSSA	1986-1992	5.3	1.1
NUS 08-7	1382-2008	1.9	4.1
WDC06A	-50-2005	3.2	1.1
IND25B5	1902-2006	7.6	0.9
TA192A	1998-2014	6.5	1.1

Table S6: Percentage of annual precipitation for the summer, from December to February (“DJF”), the autumn, from March to May (“MAM”), the winter, from June to September (“JJAS”) and the spring, from October to November (“ON”), within each year from 1998 to 2014 simulated by ERA-interim.

Year	DJF	MAM	JJAS	ON
1998	36.3	29.8	27.1	6.8
1999	26.5	22.4	38.3	12.8
2000	20.1	17.4	48.7	13.8
2001	23.6	36.4	31.2	8.7
2002	34.2	21.2	34.8	9.8
2003	30.8	15.1	47.0	7.1
2004	19.9	32.2	42.5	5.4
2005	20.1	21.3	28.5	30.2
2006	27.3	39.9	25.5	7.3
2007	25.0	37.9	29.2	8.0
2008	19.6	33.9	37.2	9.4
2009	22.7	26.8	47.2	3.3
2010	33.1	22.4	27.5	17.0
2011	38.7	18.6	25.4	17.3
2012	19.0	22.7	48.9	9.3
2013	37.7	23.6	33.4	5.4
2014	33.5	35.6	26.0	5.0

S7: Mean seasonal amplitude (“ μ ”, in ‰) and standart deviation (“ σ ”, in ‰) of $\delta^{18}\text{O}$ and deuterium excess (“dxs”) from precipitation data from our database

Site	Monitoring / recorded period	$\mu(\delta^{18}\text{O})$	$\sigma(\delta^{18}\text{O})$	$\mu(\text{dxs})$	$\sigma(\text{dxs})$
Vernadsky	1964-2013	9.0	2.0	21.4	9.6
Halley	1965-2014	16.3	4.1	17.2	8.6
Marsh	1990-1991	10.7	3.4	23.8	0.8
Rothera	1996-2014	9.8	2.7	16.7	7.6
Neumayer	1981-2000	19.9	5.6	17.7	6.8
Dome F	2003-2004	33.7	15.3	94.2	25.3
Dome C	2007-2010	31.4	11.0	67.0	14.8
GIP	2000-2007	15.1	3.6	17.8	16.2
BI	1996-2014	9.7	2.9	6.3	3.0
KM	1995-2014	7.0	3.0	5.5	2.4
KC	1958-2012	1.9	1.4	2.7	1.3
DSSA	1986-1992	8.0	2.8	5.3	1.0
NUS 08-7	1382-2008	0.8	1.1	1.9	1.7
WDC06A	-50-2005	1.8	1.1	3.2	1.0
IND25B5	1902-2006	4.4	2.1	7.6	6.4
TA192A	1998-2014	8.6	2.1	6.5	2.8

S8: ECHAM5-wiso outputs simulated from the 6th to the 08th of May in 2007 and averaged over the period 1979-2013: 2-meter temperature (2m-T, in °C), precipitation (in mm w.e. month⁻¹), zonal wind component (in m s⁻¹), meridional wind component (in m s⁻¹), the geopotential height at 500 hPa (z500, in m), the $\delta^{18}\text{O}$ (in ‰) and the d-excess (in ‰). Outputs simulated the 07th of May are highlighted using italic and bold formats.

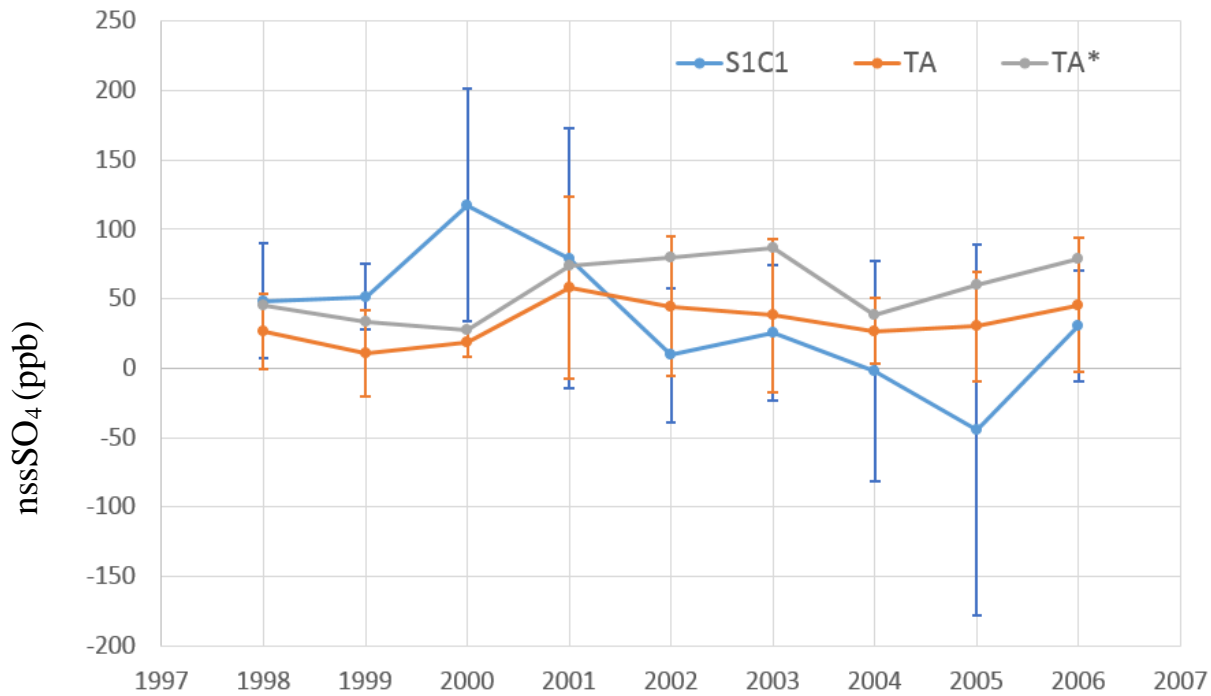
Date	Prec.		u10 (m s ⁻¹)	v10 (m s-1)	z500 (m)	$\delta^{18}\text{O}$ (‰)	d-excess (‰)
	2m-T (°C)	(mm w.e. month ⁻¹)					
06/05/2007	-21.3	0.9	-0.5	6.2	4870.8	-21.6	13.4
<i>07/05/2007</i>	<i>-22.4</i>	<i>0.2</i>	<i>-0.8</i>	<i>3.4</i>	<i>4897.0</i>	<i>6.2</i>	<i>43.3</i>
08/05/2007	-20.8	0.1	0.3	6.6	5014.5	-13.7	9.1
06/05 1979-2013	-23.7	40.4	-2.4	7.2	4970.3	-24.4	8.0
<i>07/05 1979-2013</i>	<i>-23.0</i>	<i>50.8</i>	<i>-2.7</i>	<i>7.0</i>	<i>4994.3</i>	<i>-22.1</i>	<i>7.9</i>
08/05 1979-2013	-22.0	66.4	-2.6	6.9	5002.6	-22.0	5.9

5

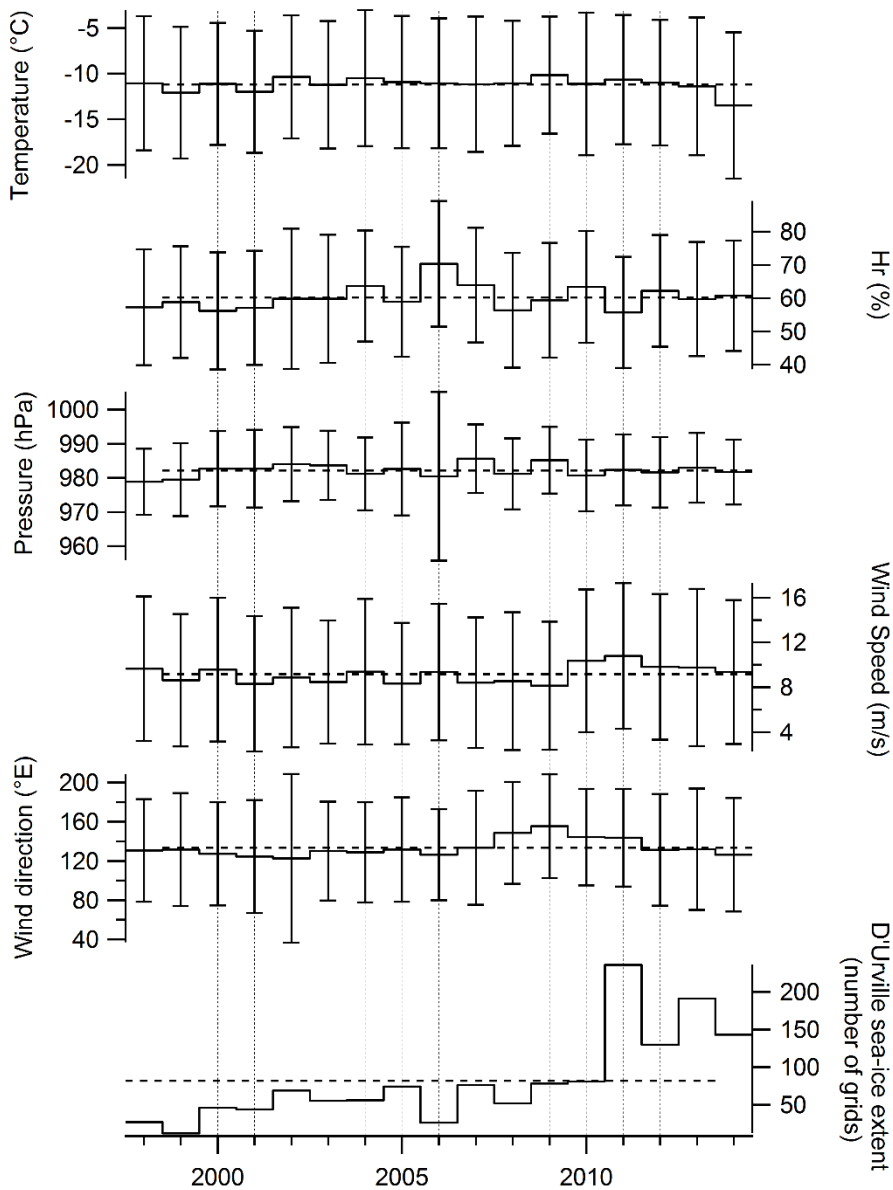
Table S9: Mean values of Na⁺ (in ppb), non sea-salt sulfate based on summer fractionation only (“nssSO₄”) (in ppb) and methane sulfonate (“MSA”) (in ppb), recorded in the S1C1 and the TA192A firn core (“TA”), as well as the ratio of the TA/S1C1 mean values ratio. Numbers into bracket correspond to the standard deviations.

	Na ⁺ (ppb)	nssSO ₄ (ppb)	MSA (ppb)
S1C1	395.6 (± 154.7)	34.9 (± 33.2)	5.2 (± 3.6)
TA	284.6 (± 124.5)	44.3 (± 13.9)	2.6 (± 1.6)
TA/S1C1 ratio	0.7	0.8	0.5

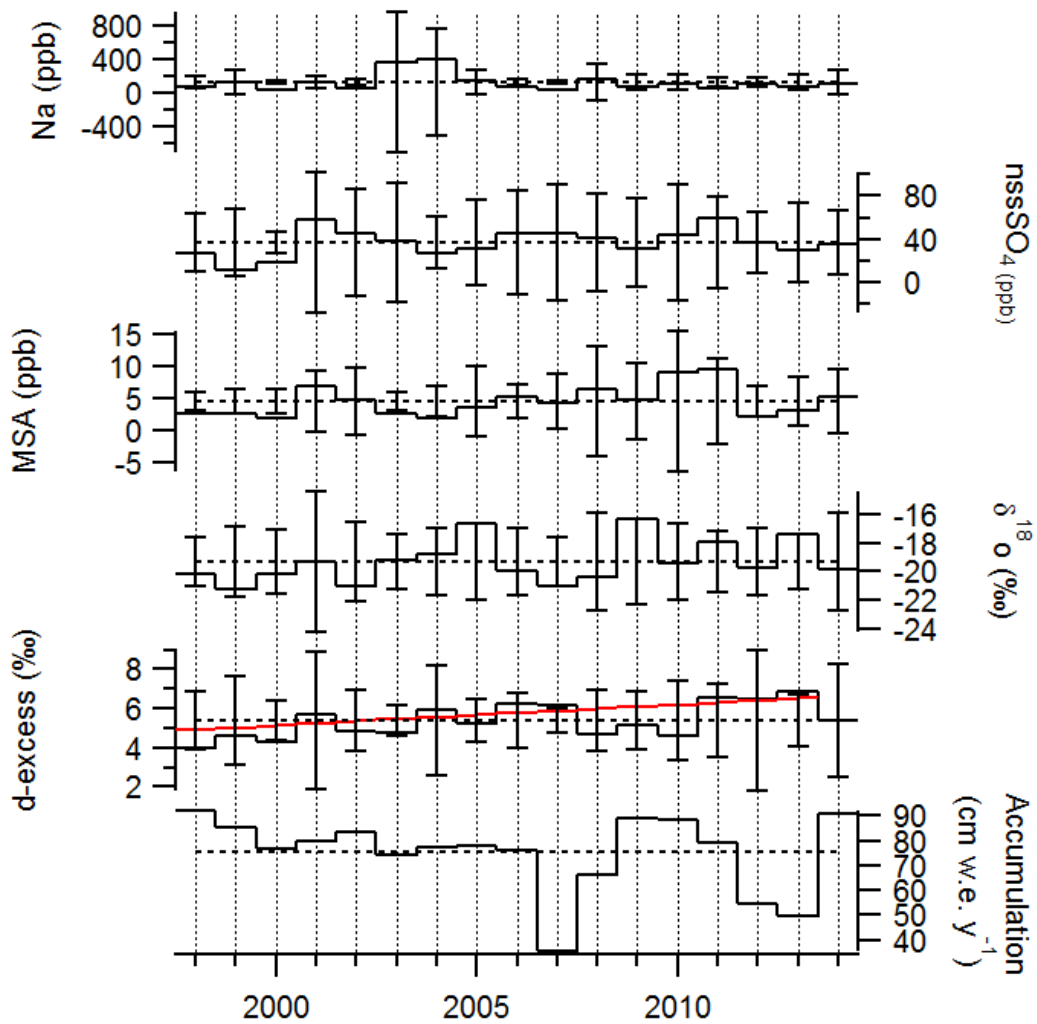
5



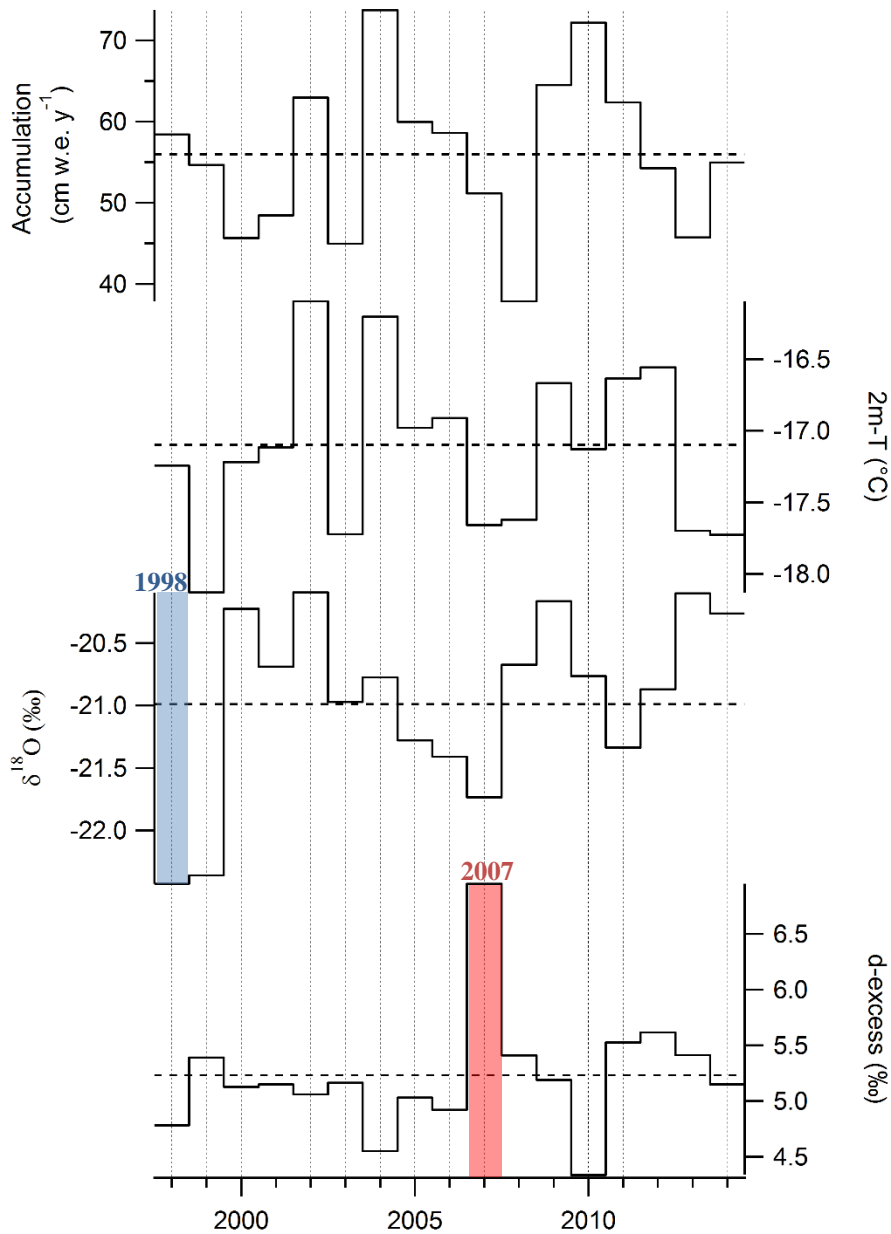
5 **Figure S1: Non sea-salt sulfate (“nssSO₄”, in ppb) measured along the S1C1 firn core, the TA192A firn core (“TA”) based on summer fractionation only and along the TA192A firn core based on summer fractionation for spring to summer seasons and winter fractionation for autumn to winter seasons (“TA*”), over their common period 1998-2006. Vertical lines correspond to standard deviation (± 1).**



5 **Figure S2: Meteorological time series over the period 1998-2014 averaged at the inter-annual scale. Near-surface temperature (in °C). Relative humidity (in %). sea level pressure (in hPa). wind speed (in m/s) and direction (°E) were provided by Meteo France. The local sea-ice concentration (in %) is extracted in the 135°E-145°E sector (with a latitudinal range of 50°S-90°S) from the Nimbus-7 Scanning Multichannel Microwave Radiometer (SMMR) and Defense Meteorological Satellite Program Special Sensor Microwave/Imagers - Special Sensor Microwave Image/Sounder (DMSP SSM/I-SSMIS) passive microwave data (Cavalieri et al., 1996). Horizontal dashed lines correspond to the climatological averages over 1998-2014 while the vertical solid lines correspond to the standard deviations.**



5 Figure S3: Dated TA192A ice core annually averaged records over the period 1998-2014: accumulation (in cm w. e. y^{-1}), concentrations of Na^+ (in ppb), $nssSO_4$ (in ppb), MSA (in ppb), $\delta^{18}O$ (in ‰) and d-excess (in ‰). Horizontal dashed lines correspond to 1998-2014 average values and vertical bars indicate the intra-annual standard deviation from resampled values.



5 **Figure S4: Time series of the simulated accumulated (i.e. precipitation minus evaporation, in cm w.e. y⁻¹), 2-meter temperature (“2m-T”, in °C), precipitated δ¹⁸O (in ‰) and precipitated d-excess (in ‰), by the ECHAM5-wiso model at the annual scale over the period 1998 – 2014. Shaded vertical lines show outstanding years (i.e. associated with values out of the range defined by mean ± 2 x standard deviation). Shading is in red when higher than the upper bound of this range, while it is in blue when lower than the inferior bound.**

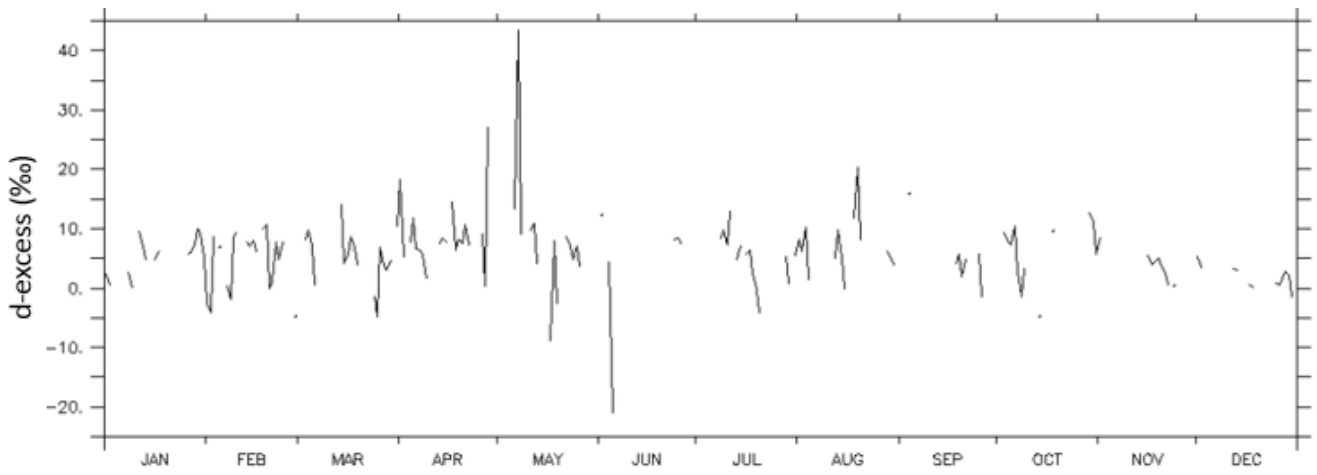


Figure S5: ECHAM5-wiso deuterium excess (“d-excess”, in ‰) at the daily scale over the whole year 2007.

(b)

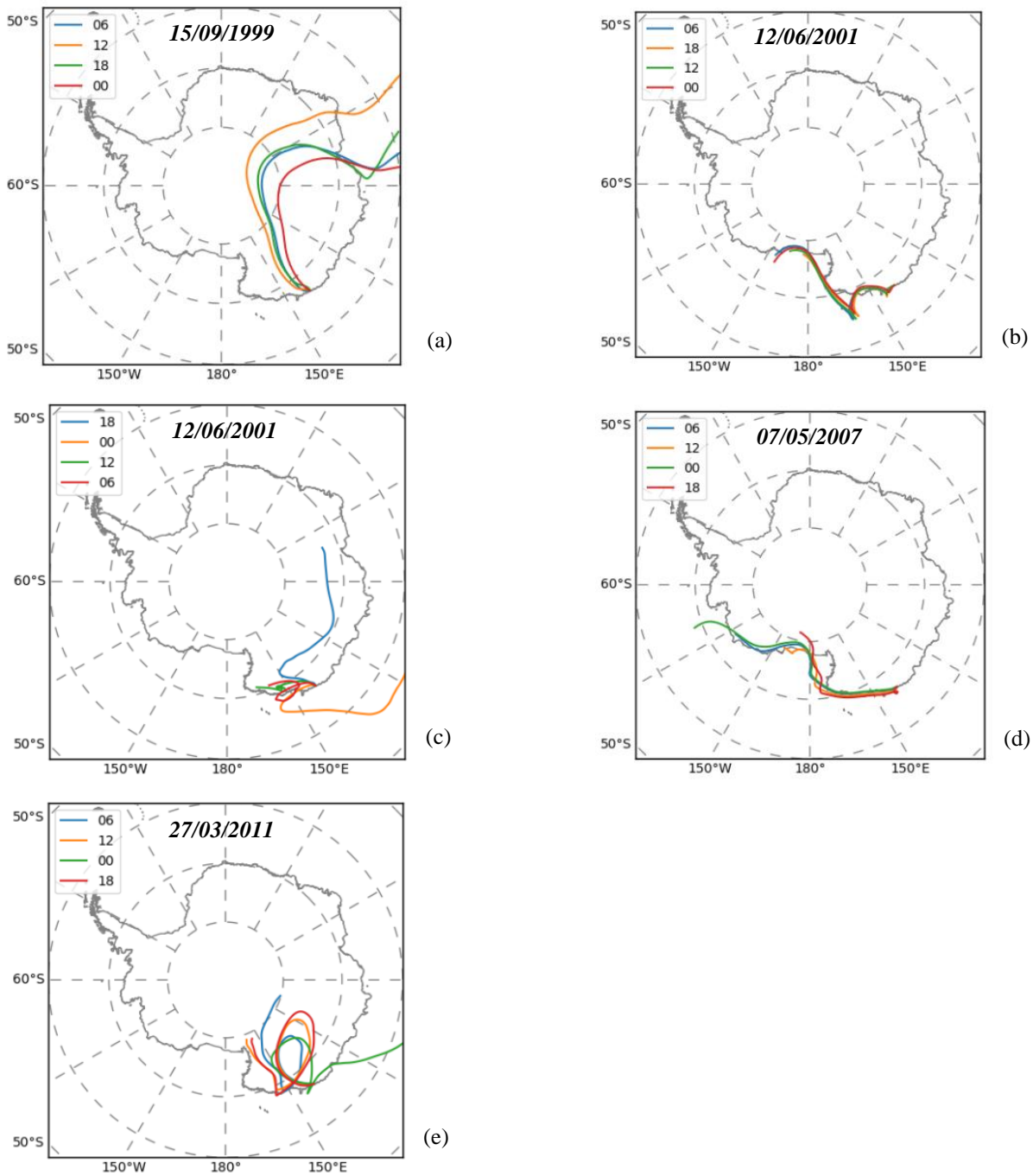


Figure S6: What drives the extreme deuterium excess values ($> 30 \text{ ‰}$) simulated by the ECHAM5-wiso? 5-days backtrajectories simulated by HYSPLIT towards the TA192A drilling site and arriving on the 15/05/1999 (a), 12/06/2001 (b), 26/02/2005 (c), 07/05/2007 (d) and 27/03/2011 (e), when deuterium excess values are higher than 40 ‰ in ECHAM5-wiso over the period 1999-2014.

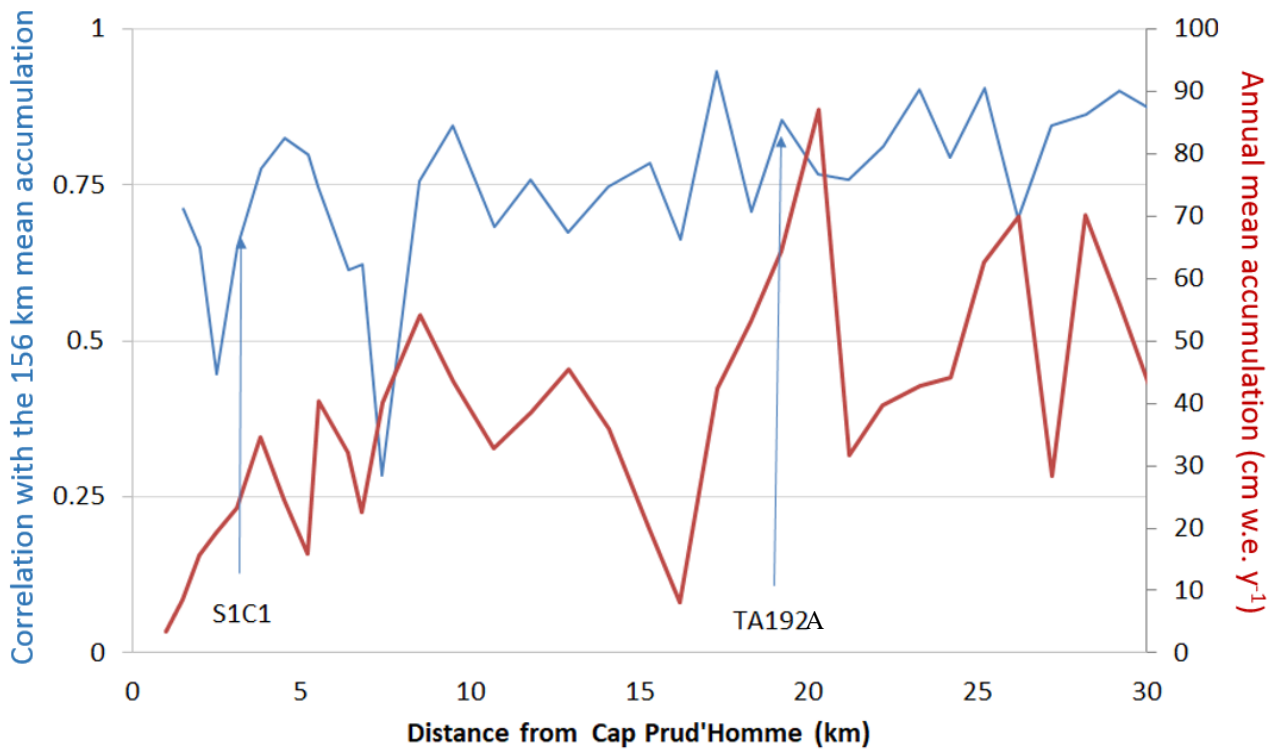
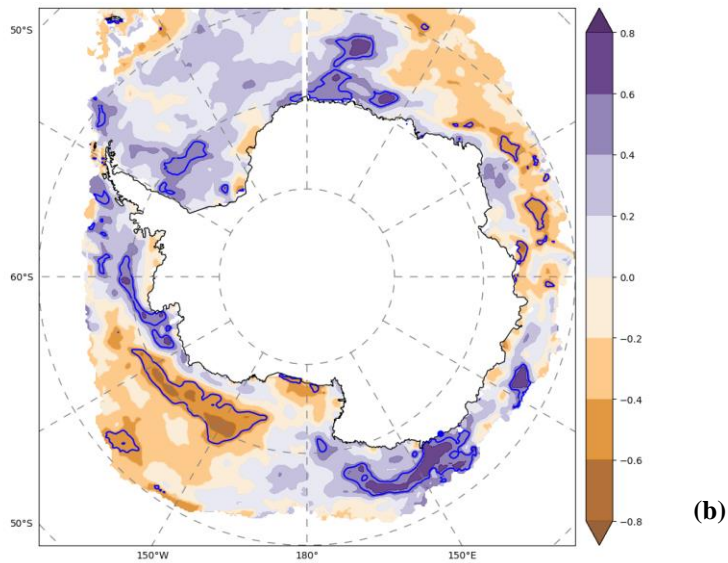
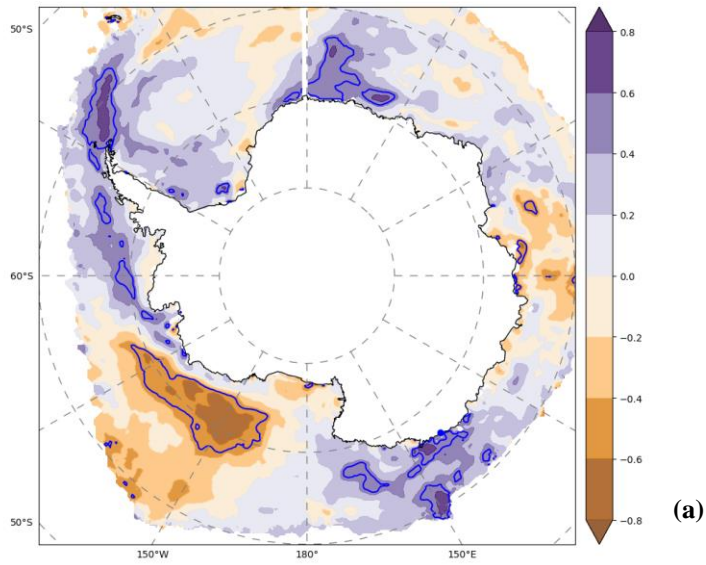


Figure S7: Annual mean accumulation of each stake data (red line) and its correlation coefficient with the 156 km mean accumulation (cm w.e. y⁻¹, blue line). The positions of the closest stake data of the S1C1 and TA192A firn cores are indicated by blue arrows.



5 **Figure S8: Correlation coefficient between annual $d\text{-exces}_{TA}$ and sea-ice concentrations (a), and between $d\text{-exces}_{TA}$ and summer sea-ice concentrations (b) over the period 1998-2014. Sea ice concentrations are extracted from the Nimbus-7 Scanning Multichannel Microwave Radiometer (SMMR) and Defense Meteorological Satellite Program Special Sensor Microwave/Imagers - Special Sensor Microwave Image/Sounder (DMSP SSM/I-SSMIS) passive microwave data (<http://nsidc.org/data/nsidc-0051>). Significant linear relationships are circled by blue lines.**

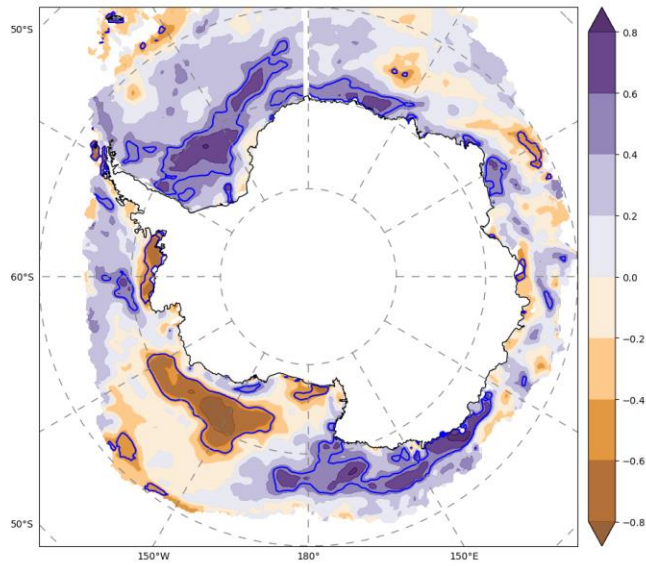
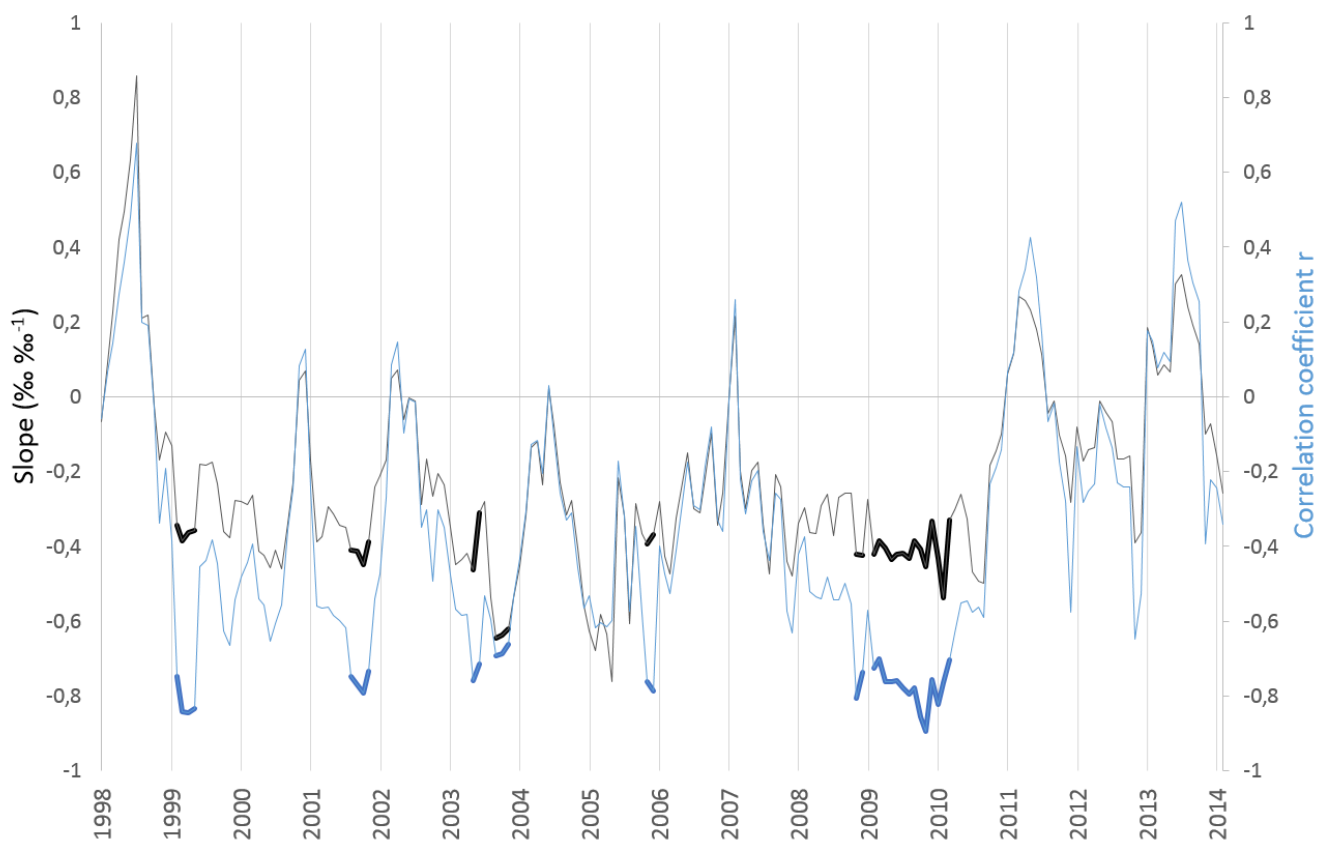


Figure S9: Correlation coefficients of Summer Sea ice concentration extracted from the Nimbus-7 Scanning Multichannel Microwave Radiometer (SMMR) and Defense Meteorological Satellite Program Special Sensor Microwave/Imagers - Special Sensor Microwave Image/Sounder (DMSP SSM/I-SSMIS) passive microwave data (<http://nsidc.org/data/nsidc-0051>). Significant linear relationships are circled by blue lines.



5

Figure S10: Slope (‰ ‰⁻¹) and correlation coefficient of the running d-excess versus $\delta^{18}\text{O}$ linear regressions over 10 points based on the $\delta^{18}\text{O}$ and d-excess simulated in the precipitation by the ECHAM5-wiso model. at the corresponding grid point to the TA192A drilling site. Only the results of the significant relationships are given. The date associated with the results correspond to the first point of the regression.

10